

Reducing the state-space of the  
complex Lorenz flow  
NSF REU summer 2009 project  
University of Chicago

Rebecca Wilczak (adviser: Predrag Cvitanović)

August 21, 2009

# Contents

<b>1</b>	<b>Complex Lorenz flow</b>	<b>4</b>
1.0.1	Visualizing complex Lorenz flow	5
1.1	Linear stability	5
1.2	Equilibria	6
1.2.1	Stability of equilibria	6
1.3	Symmetries of dynamics	7
1.4	Relative equilibria	8
1.4.1	Equations in the polar form	8
1.4.2	Computing and plotting the relative equilibrium $Q_1$	9
1.4.3	Eigen-system of the polar stability matrix	11
1.5	Reduced state space	11
1.5.1	Method of moving frames, finite time steps	12
1.5.2	Method of moving frames, differential formulation	13
1.5.3	Integration on the cross-section	15
1.6	Conclusions	16
<b>2</b>	<b>Exercises</b>	<b>18</b>
2.1	Complex Lorenz flow	18
2.2	Linear stability	19
2.3	Equilibria	19
2.4	Symmetries of dynamics	20
2.5	Relative equilibria	22
2.6	Reduced state space	26
<b>3</b>	<b>Open problems</b>	<b>31</b>
3.1	Complex Lorenz equations odds & ends	31
3.1.1	$SO(2)$ invariants of complex Lorenz equations	31
3.2	A flow with two Fourier modes	32
3.2.1	Visualizing 2-mode system	33
3.3	Linear stability	33
3.4	Symmetries of dynamics	33
3.4.1	Rotational equivariance of 2-mode system	33
3.5	Equilibria	34
3.6	Relative equilibria	34

*CONTENTS*

---

3.6.1	Equations in the polar form . . . . .	34
3.6.2	Computing and plotting the relative equilibrium $Q_1$ . . .	34
3.6.3	Eigenvalues and eigenvectors of the stability matrix . . .	35

# Chapter 1

## Complex Lorenz flow

This project first reproduces results reported by Siminos [1], and then investigates various ways of ‘quotienting’ the  $SO(2)$  symmetry of complex Lorenz equations, and reducing the dynamics to symmetry 4-dimensional reduced state space.

The project consists of my notes and exercises. The flow of the argument is in the classical **Socratic dialogue** mode; question, answer, question,  $\dots$ .

The complex Lorenz equations were introduced by Gibbon and McGuinness [2] as a low-dimensional model of baroclinic instability in the atmosphere. In the complex form, they are given by

$$\begin{aligned}\dot{x} &= -\sigma x + \sigma y \\ \dot{y} &= (r - z)x - ay \\ \dot{z} &= \frac{1}{2}(xy^* + x^*y) - bz\end{aligned}\tag{1.1}$$

where  $x, y, r = r_1 + i r_2, a = 1 + i e$  are complex and  $z, b, \sigma$  are real. Rewritten in terms of real variables  $x = x_1 + i x_2, y = y_1 + i y_2$ , complex Lorenz equations are a 5-dimensional first order ODE system [1]

$$\begin{aligned}\dot{x}_1 &= -\sigma x_1 + \sigma y_1 \\ \dot{x}_2 &= -\sigma x_2 + \sigma y_2 \\ \dot{y}_1 &= (r_1 - z)x_1 - r_2 x_2 - y_1 - e y_2 \\ \dot{y}_2 &= r_2 x_1 + (r_1 - z)x_2 + e y_1 - y_2 \\ \dot{z} &= -bz + x_1 y_1 + x_2 y_2.\end{aligned}\tag{1.2}$$

In all numerical calculations that follow we shall set the parameters to the Siminos values [1],

$$r_1 = 28, b = \frac{8}{3}, \sigma = 10, e = \frac{1}{10}, \text{ and } r_2 = 0.\tag{1.3}$$

Here we are not interested in the physical applications of these equations; rather, we study them as a simple example of a dynamical system with continuous (but no discrete) symmetries. Our goal is to find computationally straightforward method of reducing the dynamics to a lower-dimensional state space, where each group orbit of the full system (i.e., set of translationally equivalent states) is represented by a single point. If successful, the methods that we develop might be applicable to very high-dimensional flows, such as translationally equivariant fluid flows bounded by pipes or planes [3, 4].

**Acknowledgments.** R.W. and P.C. thank the James Franck Institute, U. of Chicago, for hospitality. P.C. thanks Argonne National Laboratory and Glen Robinson Jr. for support. This work was supported in parts by the National Science Foundation grants DMR 0820054, and NSF REU program DMS 0807574.

### 1.0.1 Visualizing complex Lorenz flow

In exercise 2.1 we simulate complex Lorenz flow in order to visualize its long-time dynamics, as in figure 1.1. The dynamics is a big mess - the trajectory seems to oscillate while drifting around  $z$ -axis. Of most importance in figure 1.1, is to notice that the flow has a rotational symmetry about the  $z$ -axis. Throughout the rest of the project we will try to find more illuminating ways of understanding the dynamics of this flow as well as ways of "cleaning it up"—that is, removing this symmetry and reducing the ODE system from five dimensions to four.

exercise 2.1

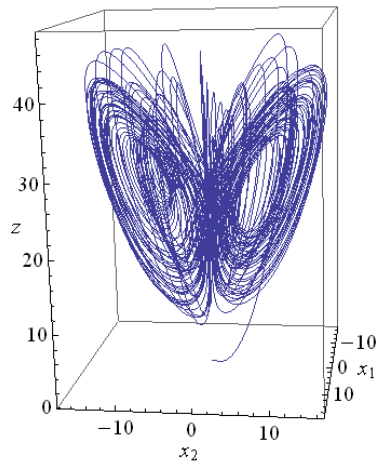


Figure 1.1: A typical  $\{x_1, x_2, z\}$  plot of the complex Lorenz flow strange attractor, with initial point  $(x_1, x_2, y_1, y_2, z) = (1, 0, 0, 1, 1)$ .

## 1.1 Linear stability

In our first attempt to understand the dynamics of the flow, we examine its stability by finding the stability matrix  $A$ . This is the matrix of partial derivatives

of  $v(x)$ ,

$$\mathbb{A} = \frac{\partial v}{\partial x} = \begin{pmatrix} \frac{\partial \dot{x}_1}{\partial x_1} & \frac{\partial \dot{x}_1}{\partial x_2} & \frac{\partial \dot{x}_1}{\partial y_1} & \frac{\partial \dot{x}_1}{\partial y_2} & \frac{\partial \dot{x}_1}{\partial z} \\ \frac{\partial \dot{x}_2}{\partial x_1} & \frac{\partial \dot{x}_2}{\partial x_2} & \frac{\partial \dot{x}_2}{\partial y_1} & \frac{\partial \dot{x}_2}{\partial y_2} & \frac{\partial \dot{x}_2}{\partial z} \\ \frac{\partial \dot{y}_1}{\partial x_1} & \frac{\partial \dot{y}_1}{\partial x_2} & \frac{\partial \dot{y}_1}{\partial y_1} & \frac{\partial \dot{y}_1}{\partial y_2} & \frac{\partial \dot{y}_1}{\partial z} \\ \frac{\partial \dot{y}_2}{\partial x_1} & \frac{\partial \dot{y}_2}{\partial x_2} & \frac{\partial \dot{y}_2}{\partial y_1} & \frac{\partial \dot{y}_2}{\partial y_2} & \frac{\partial \dot{y}_2}{\partial z} \\ \frac{\partial \dot{z}}{\partial x_1} & \frac{\partial \dot{z}}{\partial x_2} & \frac{\partial \dot{z}}{\partial y_1} & \frac{\partial \dot{z}}{\partial y_2} & \frac{\partial \dot{z}}{\partial z} \end{pmatrix} \quad (1.4)$$

**exercise 2.2** For the complex Lorenz equations it is the  $[5 \times 5]$  matrix,

$$\mathbb{A} = \begin{pmatrix} -\sigma & 0 & \sigma & 0 & 0 \\ 0 & -\sigma & 0 & \sigma & 0 \\ r_1 - z & -r_2 & -1 & -e & -x_1 \\ r_2 & r_1 - z & e & -1 & -x_2 \\ y_1 & y_2 & x_1 & x_2 & -b \end{pmatrix} \quad (1.5)$$

As explained in ChaosBook.org [5], a stability matrix describes the instantaneous rate of shearing of the infinitesimal neighborhood of  $x(t)$  by the flow. That is, it describes how quickly points initially very near to  $x(t)$  will diverge away from it in time. It is the matrix of velocity gradients. This matrix  $\mathbb{A}$  is also an important tool which we will use later on.

## 1.2 Equilibria

An equilibrium  $E$  is a point  $x_E$  for which the velocity field of an ordinary differential equation  $\dot{x} = v(x)$  is zero,  $v(x_E) = 0$ . These are points where the flow does not move, and if it reaches an equilibrium, the flow remains there. For the complex Lorenz equations the only equilibrium we found was at the origin  $E_0 = (0, 0, 0, 0, 0)$ . If we could set this *infinitely precisely* as the initial point of the flow, instead of seeing the messiness of figure 1.1, we would stay at this single point for all times. In any simulation, the (finite precision) trajectory eventually leaves this point.

**exercise 2.3**

### 1.2.1 Stability of equilibria

At an equilibrium, the flow manages to stay at a single point, but what if we start at points near the equilibrium? Will they collapse into the equilibrium, or will they diverge away from it? In order to answer this, we find and examine the eigenvalues and eigenvectors of  $\mathbb{A}$  evaluated at the equilibrium  $E_0$ . For the complex Lorenz equations we find that the eigenvalues are

**exercise 2.4**

$$\begin{aligned} \lambda_{1,2} &= 11.8277 \pm 0.062985i \\ \lambda_{3,4} &= -22.8277 \pm 0.037015i \\ \lambda_5 &= -2.66667 \end{aligned} \quad (1.6)$$

with the associated eigenvectors

$$\begin{aligned} e_1 &= e_2^* = (0.001321 + 0.4581i, 0.4581 - 0.001321i, i, 1, 0) \\ e_3 &= e_4^* = (0.002249 - 0.7795i, -0.7795 - 0.002249i, 2.8421 + i, 1, 0) \\ e_5 &= (0, 0, 0, 0, 1). \end{aligned} \tag{1.7}$$

By examining the eigensystem, we can get a sense of what happens to points near the equilibrium  $E_0$ . The numerical values of the real parts of the eigenvalues determine how quickly the flow will converge onto or diverge away from the equilibrium. For a positive real part the flow will diverge, and for a negative real part it will converge. Complex eigenvalues also indicate that the motion will be spiraling.

For the complex Lorenz equations equilibrium  $E_0$ , the values of the imaginary parts are orders of magnitude smaller than the real parts, so that there will be very little spiraling. The large values of the real parts tell us that the flow will diverge/converge from the equilibrium very quickly.

exercise 2.5

To illustrate this, we plot the eigenvectors (as real and imaginary parts) and the flow at initial points very close to  $E_0$ . The two real vectors (corresponding to a single complex eigenvector) define the plane in which the flow will spiral. We initiate the flow very close to  $E_0$  at a point along one of these vectors. In figure 1.2, we can see that for the vectors with a very small imaginary part and a positive real part, the flow does not spiral noticeably and that it diverges away from the equilibrium very quickly.

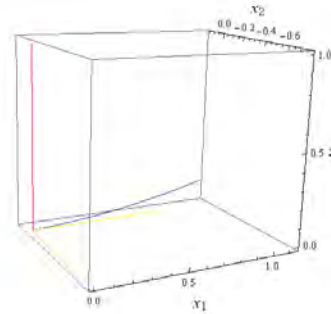


Figure 1.2:  $\{x_1, x_2, z\}$  plot of the expanding eigenvector  $e_1$  (red) and the contracting eigenvector  $e_4$  (yellow) of the equilibrium  $E_0$  stability matrix of complex Lorenz flow, with initial point at  $\frac{1}{100}e_4$ .

### 1.3 Symmetries of dynamics

In order to eventually remove the rotational symmetry in the complex Lorenz flow we need to show that the flow is rotationally equivariant. By showing this, we will then be able to apply algorithms to remove the symmetry. Rotational equivariance in this situation will let us commute a rotation operator with taking time derivatives.

We begin by defining ‘equivariance.’ A flow  $\dot{x} = v(x)$  is equivariant under an operation  $\mathbb{G}$  when

$$\mathbb{G} \cdot v(x) = v(\mathbb{G} \cdot x). \quad (1.8)$$

A Lie group element relating different state space points by a linear continuous symmetry operation can be written as

$$\mathbb{G}(\theta) = e^{i\theta\mathbb{T}}. \quad (1.9)$$

**exercise 2.6** For an infinitesimal rotation,  $\theta \ll 1$ ,

$$\mathbb{G}(\theta) = 1 + i\theta\mathbb{T} + \dots,$$

the statement of equivariance  $\dot{x} = \mathbb{G}^{(-1)} \cdot v(\mathbb{G} \cdot x)$  becomes

$$\dot{x} = (1 - i\theta\mathbb{T}) \cdot v(x + i\theta\mathbb{T} \cdot x) + \dots = v(x) - i\theta \left( \mathbb{T} \cdot v(x) - \frac{dv}{dx} \cdot \mathbb{T} \cdot x \right) + \dots.$$

The  $\dot{x}$  and  $v(x)$  cancel, and the  $i\theta$  can be divided out. We are left with the *infinitesimal rotations* version of the equivariance condition (1.8):

$$0 = -\mathbb{T} \cdot v(x) + \mathbb{A} \cdot \mathbb{T} \cdot x, \quad (1.10)$$

where  $\mathbb{A} = \frac{\partial v}{\partial x}$  is the stability matrix (1.4).

We have used both this infinitesimal rotation condition and the finite angle rotation condition (1.8), to verify that the complex Lorenz equations are rotationally equivariant.

**exercise 2.7**  
**exercise 2.8**  
**exercise 2.9**

## 1.4 Relative equilibria

To further visualize the drifting of the flow around the  $z$ -axis, we next find and plot the relative equilibria of the complex Lorenz equations. A relative equilibrium is a solution of the flow which appears stationary in a frame rotating at the appropriately chosen constant angular velocity. We find these points in a manner similar to finding the equilibria, with one difference. As the flow drifts (rotates), a relative equilibrium will drift as well, so that instead of setting all of the  $v(x) = 0$ , we allow the component of  $v(x)$  tangent to direction of group rotation to be non-zero. This tangent is not necessarily easily defined in the Cartesian coordinates which we have so far been using. The relative equilibrium is more conveniently determined in polar coordinates.

### 1.4.1 Equations in the polar form

We can rewrite the complex Lorenz equations to polar coordinates using the definition

$$(x_1, x_2, y_1, y_2, z) = (\rho_1 \cos \theta_1, \rho_1 \sin \theta_1, \rho_2 \cos \theta_2, \rho_2 \sin \theta_2, z), \quad (1.11)$$

and come up with the new equations

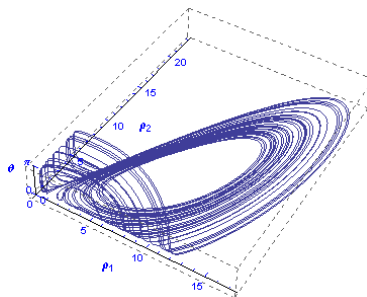
$$\begin{pmatrix} \dot{\rho}_1 \\ \dot{\theta}_1 \\ \dot{\rho}_2 \\ \dot{\theta}_2 \\ \dot{z} \end{pmatrix} = \begin{pmatrix} -\sigma(\rho_1 - \rho_2 \cos \theta) \\ -\sigma \frac{\rho_2}{\rho_1} \sin \theta \\ -\rho_2 + \rho_1((r_1 - z) \cos \theta - r_2 \sin \theta) \\ e + \frac{\rho_1}{\rho_2}((r_1 - z) \sin \theta + r_2 \cos \theta) \\ -bz + \rho_1 \rho_2 \cos \theta \end{pmatrix},$$

We know from classical mechanics that for translationally or rotationally invariant flows the relative distance is invariant (that is why one speaks of ‘relative’ equilibria), hence we introduce a variable  $\theta = \theta_1 - \theta_2$ . This is the variable which allows us to ultimately find the relative equilibria. As the flow is rotating,  $\theta_1$  and  $\theta_2$  are changing, but, at the relative equilibria, the difference between them is constant. This new variable also allows us to rewrite the complex Lorenz equations yet again, this time in only four dimensions.

exercise 2.10  
exercise 2.11

$$\begin{pmatrix} \dot{\rho}_1 \\ \dot{\rho}_2 \\ \dot{\theta} \\ \dot{z} \end{pmatrix} = \begin{pmatrix} -\sigma(\rho_1 - \rho_2 \cos \theta) \\ -\rho_2 + (r_1 - z)\rho_1 \cos \theta \\ -e - \left(\sigma \frac{\rho_2}{\rho_1} + (r_1 - z) \frac{\rho_1}{\rho_2}\right) \sin \theta \\ -bz + \rho_1 \rho_2 \cos \theta \end{pmatrix} \quad (1.12)$$

Figure 1.3: A polar coordinates  $\{\rho_1, \rho_2, \theta\}$  plot of the complex Lorenz flow strange attractor.  $\theta$  is very small until the trajectory approaches either  $\rho_1 \rightarrow 0$  or  $\rho_2 \rightarrow 0$ , where *Mathematica* continues through the singularity by a rapid change of  $\theta$  by  $\pi$ .  $\rho_1 = \rho_2 = 0$  separates the two folds of the attractor.



Plotting these equations, we see that the polar representation introduces singularities into what initially was a smooth flow, as shown in figure 1.3. We shall encounter the same problem in implementing the  $x_1 = 0$  moving frames slice, see figure 1.11.

exercise 2.12

### 1.4.2 Computing and plotting the relative equilibrium $Q_1$

To compute the relative equilibria, we use a method similar to finding the equilibria. We set  $(\dot{\rho}_1, \dot{\rho}_2, \dot{\theta}, \dot{z}) = (0, 0, 0, 0)$  and solve the set of equations numerically. We find that there are 8 solutions to the system, all differing by only positive and negative signs and variations of

$$(\rho_1, \rho_2, \theta, z) = \left( \sqrt{b(r_1 - d)}, \sqrt{bd(r_1 - d)}, \pm \cos^{-1} \left( 1/\sqrt{d} \right), r_1 - d \right) \quad (1.13)$$

where  $d = 1 + e^2/(\sigma + 1)^2$ .

Figure 1.4 shows a plot of the complex Lorenz flow in polar coordinates with initial point at the relative equilibrium,  $Q_1$ . As for an equilibrium, the flow should stay at a single point (in these polar coordinates), however, numerical errors eventually accumulate and the flow leaves  $Q_1$ .

exercise 2.14

exercise 2.13

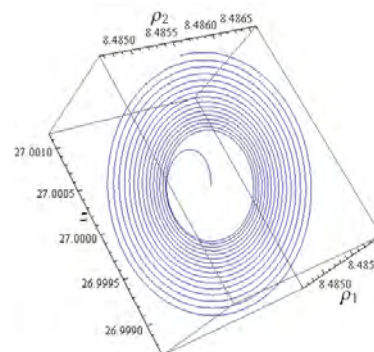


Figure 1.4:  $\{\rho_1, \rho_2, z\}$  plot of the complex Lorenz flow, with initial point at  $Q_1$ .

We can compute  $Q_1$  in Cartesian coordinates by fixing the value of  $\theta_1$  or  $\theta_2$  and using the definitions in (2.14). We get

exercise 2.15

$$x_{Q_1} = (8.48492, 0.0771356, 8.48562, 0, 26.9999).$$

Figure 1.5 shows the complex Lorenz flow with initial point at  $x_{Q_1}$ . The relative equilibrium begins by tracing out a circle around the  $z$ -axis, showing how the flow drifts. Eventually numerical errors accumulate and the circle turns into a "horn" shape when the flow begins to spiral out.

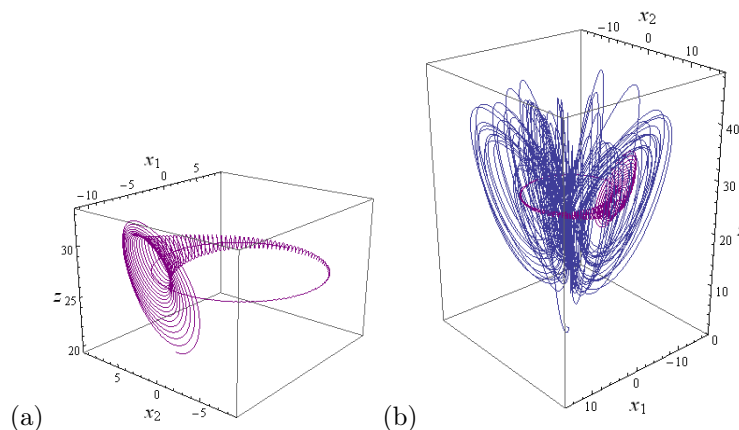


Figure 1.5: Cartesian  $\{x_1, x_2, z\}$  plot of the complex Lorenz flow (a) with initial point close to  $Q_1$ , (b) superimposed over the strange attractor of figure 1.1.

As discussed above, there are in total eight relative equilibria. Figure 1.6 shows the flow with initial point at four of these eight points and plotted in Cartesian coordinates. Each of the initial points lies on the circle. As the flow itself is rotationally invariant, all of these eight relative equilibria are equivalent. From here on, we only examine the properties of the point defined above as  $x_{Q_1}$ .

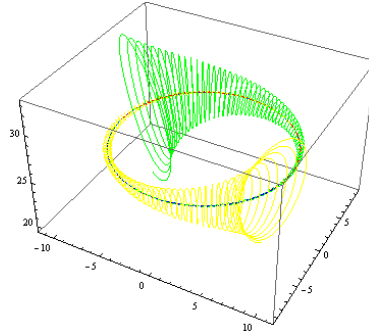


Figure 1.6: Plot of four different relative equilibrium solutions (red, yellow, green, blue). Some of the plots almost exactly overlap and are not easily distinguishable.

### 1.4.3 Eigen-system of the polar stability matrix

As in sect. 1.1, we now find and plot the eigensystem of the stability matrix in order to understand the stability of  $Q_1$ . Using the same methods described there, we find the eigenvalues

$$(\lambda_{1,2}, \lambda_3, \lambda_4) = (0.0938179 \pm 10.1945i, -11.0009, -13.8534)$$

with the eigenvectors

$$\begin{aligned} \operatorname{Re} e_1 &= \operatorname{Re} e_2 = (-0.266121, -0.0321133, 0.00034139, 0.719222) \\ \operatorname{Im} e_1 &= -\operatorname{Im} e_2 = (-0.295017, 0.569063, -0.000551886, 0) \\ e_3 &= (-0.0883591, -0.0851485, -0.989135, -0.0809553) \\ e_4 &= (-0.855586, -0.329912, -0.00273531, -0.398902). \end{aligned} \quad (1.14)$$

As in sect. 1.1, we can also plot the flow (in polar coordinates) with an initial point very near to  $Q_1$  along one of the eigenvectors. Figure 1.7 shows just this.

exercise 2.16  
exercise 2.17

## 1.5 Reduced state space

Finally, we move on to the goal of the project, reducing the state-space of the complex Lorenz equations to only four dimensions. We present two different versions of the ‘method of moving frames.’ The method can introduce singularities of the type we have encountered in the polar coordinate reformulation, as in figure 1.3. We encounter these in applying ‘polar’ version of the method, but

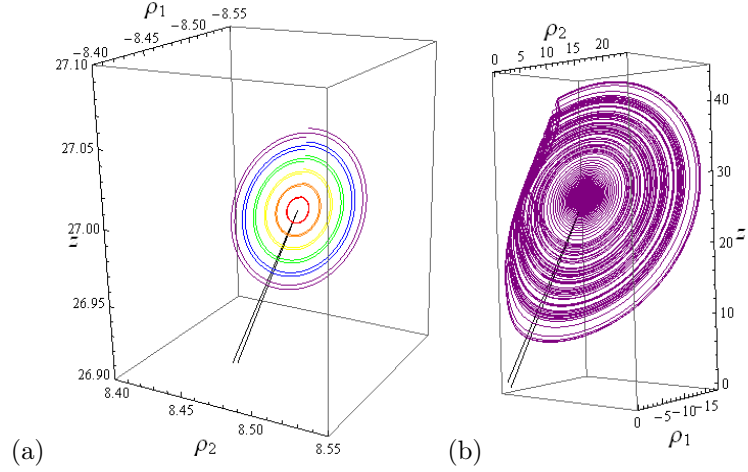


Figure 1.7: (a)  $\{\rho_1, \rho_2, z\}$  plot of the eigenvector  $e_3$  (black) and the polar complex Lorenz flow at initial values of  $\frac{1}{100}, \frac{2}{100}, \frac{3}{100}, \frac{4}{100}, \frac{5}{100}$ , and  $\frac{6}{100}$  of  $e_3$  (red, orange, yellow, green, blue, violet) with  $t$  from 0 to  $2T_{\text{spiral}} = 1.232$ , (b) with initial point at  $\frac{6}{100}e_3$  (violet) and with  $t$  from 0 to 100.

not in the other, more general version. We finish by reproducing Siminos ‘integration on the cross-section’ which - inspite of lacking a theoretical justification - projects the complex Lorenz flow to a nice Lorenz-type attractor.

This section of the report is written in collaboration with E. Siminos and P. Cvitanović.

### 1.5.1 Method of moving frames, finite time steps

exercise 2.18

Siminos [1] discusses symmetry reduction by the method of *moving frames* of Cartan [6], in the formulation of Fels and Olver [7, 8, 9]. The moving frames method allows the determination of (in general non-polynomial) invariants of the group action by a simple and efficient algorithm that, as argued in [1], works well in high-dimensional state spaces.

Split up the integration of the  $\text{SO}(2)$ -equivariant ODE into a sequence of short time steps, each followed by a rotation such that the next segment initial point is in the point  $x^*$  slice, a  $(d-1)$ -dimensional hyperplane normal to the group rotation tangent  $t^*$  at point  $x^*$ :

$$(x - x^*) \cdot t^* = 0, \quad t^* = \mathbb{T} \cdot x^*. \quad (1.15)$$

For any  $\hat{x}$ ,  $x = \mathbb{G}(\theta) \cdot \hat{x}$  is defined to be the rotation of  $\hat{x}$  that lies in the slice. Such a map from a point in space to the group action is called a *moving frame* in the formulation of Fels and Olver [7, 8, 9]. A generic point  $x^*$  not on the  $z$  axis should suffice to fix a good slice, for example a point on an relative equilibrium

exercise ?? group orbit,  $x^* = x_{Q1}$ . As  $x^* \cdot t^* = 0$  by the antisymmetry of  $\mathbb{T}$ , (1.15) reduces to the condition

$$0 = x \cdot \mathbb{T} \cdot x^* = \hat{x} \cdot \mathbb{G}(\theta)^T \cdot \mathbb{T} \cdot x^* \quad (1.16)$$

that determines  $\theta$  for a given  $\hat{x}$ . Each circle intersects the section exactly twice, so there are two solutions, separated by  $\pi$ . We select the one with a smaller clockwise rotation angle into the slice. The  $z$ -axis invariant subspace is always within the section, so this is a nice, globally transverse slice.

Figure 1.8: Method of moving frames, finite time steps version: a trajectory started on the slice, with  $x_1^{(0)} = 0$ , evolves for a finite time to a state space point with a non-zero  $\hat{x}_1^{(1)}$ . The *entire* state space is then rotated (the ‘frame is moved’) so that the equivalent point on the circle lies on the slice,  $x_1^{(1)} = 0$ . Thus after every finite time step followed by a rotation the trajectory returns to the  $4d$   $x_1 = 0$  reduced state space.

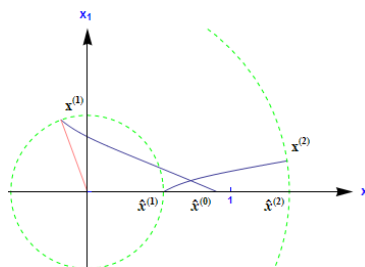


Figure 1.8 illustrates the method of moving frames, finite time version, for a slice motivated by the polar form of the complex Lorenz equations of sect. 1.4.1. It is defined, for example, by taking  $(x_1^*, x_2^*, y_1^*, y_2^*) = (0, 1, 0, 0)$ ,  $x_1 = 0$ ,  $x_2 > 0$ . Start at  $x^{(0)}$  with  $x_1^{(0)} = 0$ , evolve for a finite time to  $\hat{x}^{(1)}$ . Compute the polar angle  $\theta_1$  of  $\hat{x}^{(1)}$  in the  $(x_1, x_2)$  plane, and rotate the *entire* state space (hence ‘moving frame’) clockwise by  $\theta_1$ ,  $x^{(1)} = \mathbb{G}(\theta_1) \cdot \hat{x}^{(1)}$ , to satisfy the  $x_1 = 0$  slice condition. Repeat. The trajectory remains in the  $4d$   $x_1 = 0$  reduced state space.

## 1.5.2 Method of moving frames, differential formulation

I made a wrong mistake.

—Yogi Berra

Infinitesimal time version of the moving frames symmetry reduction is attained by taking small time steps in figure 1.8 and dropping the higher order terms, as in sect. 1.3. For infinitesimal  $d\theta$  we set  $\sin d\theta \approx d\theta$ ,  $\cos d\theta \approx 1$ ,  $\mathbb{G}(d\theta) \approx 1 + d\theta \mathbb{T}$ , and the condition (1.15) for rotating an infinitesimal time evolution step  $dx = v dt$  back into the slice

$$0 = (x + dx) \cdot \mathbb{G}(d\theta)^T \cdot \mathbb{T} \cdot x^* \approx (x + dt v) \cdot (1 + d\theta \mathbb{T})^T \cdot \mathbb{T} \cdot x^* \approx dt v \cdot \mathbb{T} \cdot x^* - d\theta x \cdot \mathbb{T} \cdot \mathbb{T} \cdot x^*$$

yields

$$d\theta \approx \frac{v \cdot \mathbb{T} \cdot x^*}{x \cdot \mathbb{T} \cdot \mathbb{T} \cdot x^*} dt. \quad (1.17)$$

exercise 2.20

exercise 2.21

exercise 2.22

exercise 2.24

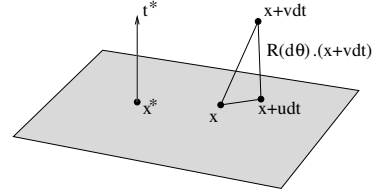


Figure 1.9: Method of moving frames, infinitesimal formulation.

Let  $u(x)$  be the vector field that generates the flow in the reduced state space. According to figure 1.9, in the limit that  $\mathbb{G}(d\theta) \approx 1 + d\theta \mathbb{T}$  the infinitesimal time step under  $u$  is connected to the time step under  $v$  by

$$x + u dt = (1 + d\theta \mathbb{T}) \cdot (x + v dt).$$

Dropping second order terms, dividing through with  $dt$

$$u = v + \frac{d\theta}{dt} \mathbb{T} \cdot \hat{x},$$

and substituting (1.17) gives the reduced state space equations:

$$\dot{x} = v - \frac{(v \cdot \mathbb{T} \cdot x^*)}{(x \cdot x^*)_4} \mathbb{T} \cdot x, \quad (1.18)$$

where we have used the fact that  $-x \cdot \mathbb{T} \cdot \mathbb{T} \cdot x^* = (x \cdot x^*)_4 = x_1 x_1^* + x_2 x_2^* + y_1 y_1^* + y_2 y_2^*$  is the dot-product restricted to the 4-dimensional representation of  $\text{SO}(2)$ . By construction, the motion stays in the  $(d-1)$ -dimensional slice.

exercise 2.23

A generic  $x^*$  can be brought to form  $x^* = (0, 1, y_1^*, y_2^*)$  by a rotation and rescaling. Then  $\mathbb{T} \cdot x^* = (1, 0, y_2^*, -y_1^*)$ , and

$$\frac{(v \cdot \mathbb{T} \cdot x^*)}{(x \cdot x^*)_4} = \frac{v_1 + v_3 y_2^* - v_4 y_1^*}{x_2 + y_1 y_1^* + y_2 y_2^*}. \quad (1.19)$$

A long time trajectory of (1.18) with  $x^*$  on the relative equilibrium  $Q_1$  group orbit is shown in figure 1.10. As initial condition we chose an initial point on the unstable manifold of  $Q_1$ , rotated back to the slice by angle  $\theta$  as prescribed by (1.16). In figure 1.10 we show the part of the trajectory for  $t \in [70, 100]$ . The relative equilibrium, now an equilibrium of the reduced state space dynamics, organizes the flow into a Rössler type attractor. There appears to be no singularity in this attractor although we can run into trouble with (1.18) wherever the denominator in (1.17) vanishes, i.e., the direction of group action on the point  $x$  is perpendicular to the direction of group action on  $x^*$ .

exercise ??

Indeed, the method appears to encounter singularities in subsets of state space [1]. For example, the reduced state space equations (1.19) for the polar coordinates inspired slice  $x^* = (0, 1, 0, 0)$ ,  $x_1 = 0$ ,  $x_2 > 0$ , are given by

exercise 2.19

$$\dot{x} = v - \frac{v_1}{x_2} \mathbb{T} \cdot x. \quad (1.20)$$

A typical trajectory is shown in figure 1.11. The problem with defining the slice by (1.20) is apparently that it fixes rotations in the  $(x_1, x_2)$  plane, not the full  $4d$  space.

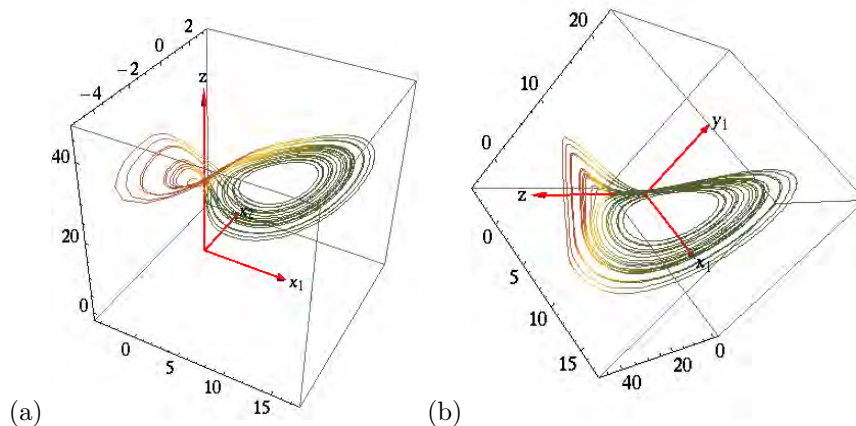


Figure 1.10: Method of moving frames, slice fixed by a point on an relative equilibrium group orbit,  $x^* = x_{Q1}$ . The strange attractor of figure 1.1 in the reduced state space of (1.18): (a)  $\{x_1, x_2, z\}$  projection, (b)  $\{x_1, y_1, z\}$  projection. Color-coding indicates  $(\hat{x} \cdot \hat{x}^*)_4$  where  $\hat{\cdot}$  stands for unit vector, with green indicating values of the inner product close to 1 and brown indicating values close to 0.

### 1.5.3 Integration on the cross-section

Our second method of symmetry reduction Siminos [1] calls *integration on the cross-section* (II). Here, we use the projection operator

$$\mathbf{P}_{ij}^\perp(x^*) = \delta_{ij} - \frac{(\mathbb{T} \cdot x^*)_i (\mathbb{T} \cdot x^*)_j}{(\mathbb{T} \cdot x^*)^2} \quad (1.21)$$

to remove any components of the complex Lorenz equations that are tangent to the rotation about the  $z$ -axis. Unlike the method of moving frames where we continually rotate points back to the slice, in this method the components of integration are tangent to the rotation only when crossing the hyperplane fixed by  $x^*$ . We define the new flow  $\frac{dx}{dt} = \mathbf{P}^\perp(x^*)v(x)$ , following Siminos [1], as

$$\dot{x}_\perp = v(x) - \mathbb{T}x^* \frac{\mathbb{T}x^* \cdot v(x)}{(\mathbb{T}x^*)^2} \quad (1.22)$$

where  $\mathbb{T}$  is the same as defined above and  $x^*$  is an arbitrary point defining the cross-section. This approach results in a nice 4-dimensional projection of the complex Lorenz flow, as Siminos showed in figure 1.12 (a). Using (2.32), we were able to reproduce this in figure 1.12 (b). However, as we were not able to establish a theoretical foundation for this projection, it remains only an interesting visualization suggested by the method of moving frames, not a viable method for symmetry reduction in its own right.

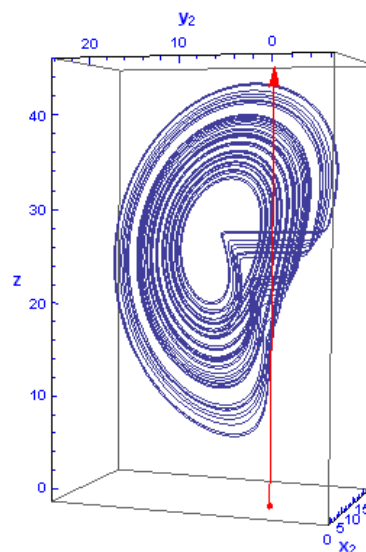


Figure 1.11: Method of moving frames, continuous time version, for the polar coordinates motivated  $x^* = (0, 1, 0, 0)$ ,  $x_1 = 0$ ,  $x_2 > 0$ , slice. The strange attractor of figure 1.1 in the reduced state space,  $\{x_2, y_2, z\}$  projection exhibits a discontinuity at  $x_2 = 0$ .

## 1.6 Conclusions

Both the method of moving frames and integration on the cross-section are still under development. We are not yet sure whether either could be considered a success or failure. The method of moving frames seems so far to produce a figure without singularities, but it would require further work to verify that singularities never occur. Integration on the cross-section also produces a smooth flow, resembling the classical Lorenz attractor, and one could use the same tools to analyze it. This method seems to work, although there is no rigorous reason why it should.

Future work should investigate in more depth the viability of the methods studied here. New methods (hopefully more successful than the ones we have tested) with which to remove the symmetry in the complex Lorenz equations and multitude of other dynamical systems with continuous symmetries need to be developed. Siminos Ph.D. thesis [1] addresses some of these issues. In this project we have discussed, understood, and tested the ‘moving frames’ method as applied to complex Lorenz equations in the thesis. Much work still remains before these are viable methods for higher-dimensional flows.

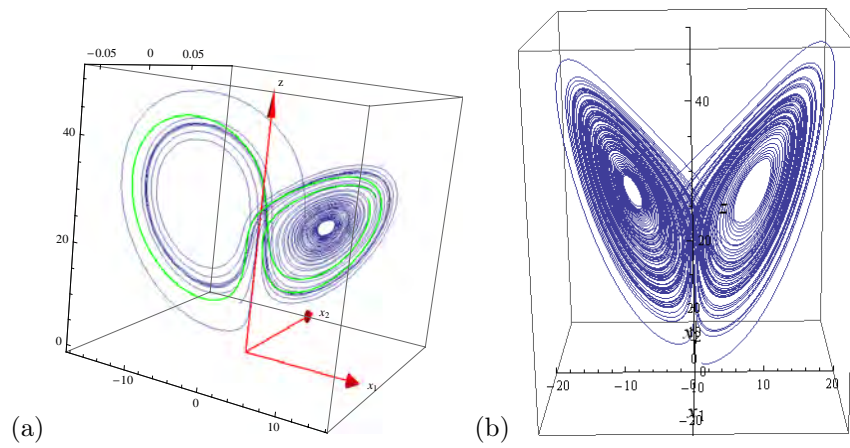


Figure 1.12: Restriction of complex Lorenz equations dynamics on the slice  $\mathcal{K}$  through (2.31). A trajectory initiated on the unstable manifold of  $Q_1$  is shown in blue and relative periodic orbit “011” is shown in green. ( $e = 1/10$ ,  $\rho_2 = 0$ ). (a) From Siminos Ph.D. thesis [1], (b) our implementation.

## Chapter 2

# Exercises

### 2.1 Complex Lorenz flow

**Exercise 2.1** *Visualizations of the 5-dimensional complex Lorenz flow:* Plot complex Lorenz flow projected on any three of the five  $\{x_1, x_2, y_1, y_2, z\}$  axes. Experiment with different visualizations.

**Solution 2.1** - *Visualizations of the 5-dimensional complex Lorenz flow.* A numerical solution of the set of ODEs (1.2) is obtained by using the Mathematica `NDSolve` function, for  $t$  from 0 to 100 and setting the initial  $(x_1, x_2, y_1, y_2, z)$  to some arbitrary value. We set `MaxSteps`  $\rightarrow$  `Infinity` in order to resolve the fine structure of the flow. The solution is then plotted by means of `ParametricPlot3D`, in any three of the five  $\{x_1, x_2, y_1, y_2, z\}$  axes. Figure 1.1 illustrates the shape of the attractor projected onto the  $\{x_1, x_2, z\}$  subspace, with parameters set to the Siminos values (1.3). Projections onto  $\{y_1, y_2, z\}$  and other subspaces are visually similar, and seem not to offer additional insights into dynamics of this system.

Here is a Mathematica program that generates a long-time plot of complex Lorenz equations, such as figure 1.1, initiated from a point on the attractor (after this integration, the initial condition `ic` is the final point of the preceding integration):

```
v[t_]={-σ x1[t] + σ y1[t], -σ x2[t] + σ y2[t],
(r1 - z[t])x1[t] - r2x2[t] - y1[t] - ey2[t],
r2x1[t] + (r1 - z[t])x2[t] + ey1[t] - y2[t],
-b z[t] + x1[t]y1[t] + x2[t]y2[t]};
x[t_] = {x1[t], x2[t], y1[t], y2[t], z[t]};
d=Length[x[t]];
eqns=Table[D[x[t][[i]],t]==v[t][[i]],{i,1,d}];
xde={x1, x2, y1, y2, z};

r1= 28; r2=0; b=8/3; e=1/10; σ=10;
tf= 80;
ic={x1[0]==0.867, x2[0]==-0.455, y1[0]==-0.552, y2[0]==0.453, z[0]==22.4};
```

```
sol=NDSolve[{eqns,ic}, xde, {t,0,tf}, MaxSteps -> Infinity//Flatten;
traj[t_]=x[t]/.sol;
p1=ParametricPlot3D[{traj[t][[1]], traj[t][[2]], traj[t][[5]]},
{t,0,tf}, PlotPoints -> 400, PlotRange -> All]
ic=Table[x[0][[i]]==traj[tf][[i]], {i,1,d}];
```

(R. Wilczak, Jun 17 2009)

## 2.2 Linear stability

**Exercise 2.2** *Stability matrix of complex Lorenz flow:* Find the stability matrix of complex Lorenz equations (1.2).

**Solution 2.2 - Stability matrix of complex Lorenz flow.** Substituting (1.2) into (1.4), Mathematica program

```
v[t] = {x1'[t], x2'[t], y1'[t], y2'[t], z'[t]};
x[t] = {x1[t], x2[t], y1[t], y2[t], z[t]};
A = D[v[t], {x[t], 1}]
```

we find

$$A = \begin{pmatrix} -\sigma & 0 & \sigma & 0 & 0 \\ 0 & -\sigma & 0 & \sigma & 0 \\ r_1 - z & -r_2 & -1 & -e & -x_1 \\ r_2 & r_1 - z & e & -1 & -x_2 \\ y_1 & y_2 & x_1 & x_2 & -b \end{pmatrix}. \quad (2.1)$$

(R. Wilczak and P. Cvitanović, Jun 19 2009)

## 2.3 Equilibria

**Exercise 2.3** *Equilibria of complex Lorenz equations:* Find all equilibria of complex Lorenz equations.

**Solution 2.3 - Equilibria of complex Lorenz equations.** To find these points for complex Lorenz equations, I used the Solve function in Mathematica, with

$$\begin{pmatrix} \dot{x}_1(t) \\ \dot{x}_2(t) \\ \dot{y}_1(t) \\ \dot{y}_2(t) \\ \dot{z}(t) \end{pmatrix} = \begin{pmatrix} \sigma y_1(t) - \sigma x_1(t) \\ \sigma y_2(t) - \sigma x_2(t) \\ -r_2 x_2(t) - y_1(t) - e y_2(t) + x_1(t)(r_1 - z(t)) \\ r_2 x_1(t) + e y_1(t) - y_2(t) + x_2(t)(r_1 - z(t)) \\ x_1(t) y_1(t) + x_2(t) y_2(t) - b z(t) \end{pmatrix} = \begin{pmatrix} 0 \\ 0 \\ 0 \\ 0 \\ 0 \end{pmatrix}$$

as the equations defining the system, and then solved for  $x_1(t), x_2(t), y_1(t), y_2(t)$ , and  $z(t)$ . Mathematica returns the point  $(0, 0, 0, 0, 0)$  as the only solution, and thus (we hope, we do not have a proof) the only equilibrium point. (R. Wilczak, Jun 22 2009)

**Exercise 2.4** *Eigenvalues and eigenvectors of  $E_0$  stability matrix:* Find the eigenvalues and the eigenvectors of the stability matrix  $\mathbb{A}$  at  $E_0 = (0, 0, 0, 0, 0)$  determined in exercise 2.3.

**Solution 2.4** - *Eigenvalues and eigenvectors of  $E_0$  stability matrix.* Using the Mathematica function *EigenSystem* and setting  $(x_1, x_2, y_1, y_2, z) = (0, 0, 0, 0, 0)$  at  $t = 0$  we obtain

$$\begin{aligned}\lambda_{1,2} &= 11.8277 \pm 0.062985i \\ \lambda_{3,4} &= -22.8277 \pm 0.037015i \\ \lambda_5 &= -2.66667\end{aligned}\tag{2.2}$$

as the eigenvalues of the system, with the associated eigenvectors:

$$\begin{aligned}e_1 = e_2^* &= (0.00132196 + 0.458131i, 0.458131 - 0.00132196i, i, 1, 0) \\ e_3 = e_4^* &= (0.00224947 - 0.779559i, -0.779559 - 0.00224947i, 2.842171 + i, 1, 0) \\ e_5 &= (0, 0, 0, 0, 1).\end{aligned}\tag{2.3}$$

(R. Wilczak, Jun 26 2009)

**Exercise 2.5** *The eigen-system of the stability matrix at  $E_0$ :* Plot the eigenvectors of  $\mathbb{A}$  at  $E_0$  and the complex Lorenz flow at values very close to  $E_0$ .

**Solution 2.5** - *The eigen-system of the stability matrix at  $E_0$ .* In order to plot the complex eigenvectors, we split them into their real and complex parts and plot each separately (so that one complex eigenvector becomes two, defining a plane). Using the same method as in the previous plotting exercises (exercise 2.1, exercise 2.14, exercise 2.15) we arrive at figure 1.2. As the eigenvalues are nearly real, the stable/unstable 2d manifolds barely spiral, and are not very illuminating.

(R. Wilczak, Jul 01 2009)

## 2.4 Symmetries of dynamics

**Exercise 2.6**  *$SO(2)$  rotations in a plane:* Show by exponentiation (1.9) that the  $SO(2)$  Lie algebra element  $\mathbb{T}$  generates rotation  $\mathbb{G}$  in a plane,

$$\mathbb{G}(\theta) = e^{i\mathbb{T}\theta} = \cos \theta \begin{pmatrix} 1 & 0 \\ 0 & 1 \end{pmatrix} + \sin \theta \begin{pmatrix} 0 & 1 \\ -1 & 0 \end{pmatrix} = \begin{pmatrix} \cos \theta & \sin \theta \\ -\sin \theta & \cos \theta \end{pmatrix}.\tag{2.4}$$

**Solution 2.6** -  *$SO(2)$  rotations in a plane.* Expand  $\exp(i\theta\mathbb{T})$  as a power series, noting that

$$\mathbb{T}^2 = \begin{pmatrix} 0 & 1 \\ -1 & 0 \end{pmatrix}^2 = -\mathbf{1}.$$

(P. Cvitanović, Jul 10 2009)

**Exercise 2.7** *Rotational equivariance of complex Lorenz equations for infinitesimal angles.* Show that complex Lorenz equations are equivariant under infinitesimal  $SO(2)$  rotations.

**Solution 2.7** - *Rotational equivariance of complex Lorenz equations for infinitesimal angles.* Now that we have the stability matrix (1.4), we can check the equivariance condition (1.10),  $0 = -\mathbb{T}v(x) + \mathbb{A}\mathbb{T}x$ , where  $\mathbb{A} = \frac{\partial v}{\partial x}$  is the stability matrix, by explicit substitution. The matrix  $\mathbb{T}$  is

$$\mathbb{T} = \begin{pmatrix} 0 & 1 & 0 & 0 & 0 \\ -1 & 0 & 0 & 0 & 0 \\ 0 & 0 & 0 & 1 & 0 \\ 0 & 0 & -1 & 0 & 0 \\ 0 & 0 & 0 & 0 & 0 \end{pmatrix}. \quad (2.5)$$

Plugging these into (1.10), as well as using (1.2) for  $v(x)$ , the result is indeed 0, as expected. Then the system is rotationally equivariant for infinitesimal angles. (R. Wilczak, Jun 21 2009)

**Exercise 2.8**  *$U(1)$  equivariance of complex Lorenz equations for finite angles:* Show that complex Lorenz equations (1.1) are equivariant under finite angle rotation (1.9).

**Solution 2.8** -  *$U(1)$  equivariance of complex Lorenz equations for finite angles.* Multiply the coordinates by a complex phase:  $x \rightarrow e^{i\theta}x$ ,  $y \rightarrow e^{i\theta}y$ . Equivariance of (1.1) follows by inspection. If all coefficients are real, there is also a discrete  $C_1$  symmetry under complex conjugation of the three equations. However, we shall consider here the cases where one or both of the parameters  $r$  and  $a$  are complex, breaking this discrete symmetry. (P. Cvitanović, Jul 9 2009)

**Exercise 2.9**  *$SO(2)$  equivariance of complex Lorenz equations for finite angles:* Show that complex Lorenz equations (1.2) are equivariant under rotation for finite angles.

**Solution 2.9** -  *$SO(2)$  equivariance of complex Lorenz equations for finite angles.* For this problem, the operation is rotation and  $v(x)$  is given by (1.2). Rotation can be defined using the matrix

$$\mathbb{G}(\theta) = \begin{pmatrix} \cos(\theta) & \sin(\theta) & 0 & 0 & 0 \\ -\sin(\theta) & \cos(\theta) & 0 & 0 & 0 \\ 0 & 0 & \cos(\theta) & \sin(\theta) & 0 \\ 0 & 0 & -\sin(\theta) & \cos(\theta) & 0 \\ 0 & 0 & 0 & 0 & 1 \end{pmatrix} \quad (2.6)$$

where  $\theta$  is the angle of rotation. We need to verify that

$$v(x) = \mathbb{G}^{-1} \cdot v(\mathbb{G} \cdot x). \quad (2.7)$$

First, the system is rotated as

$$\begin{pmatrix} \cos(\theta) & \sin(\theta) & 0 & 0 & 0 \\ -\sin(\theta) & \cos(\theta) & 0 & 0 & 0 \\ 0 & 0 & \cos(\theta) & \sin(\theta) & 0 \\ 0 & 0 & -\sin(\theta) & \cos(\theta) & 0 \\ 0 & 0 & 0 & 0 & 1 \end{pmatrix} \cdot \begin{pmatrix} x_1(t) \\ x_2(t) \\ y_1(t) \\ y_2(t) \\ z(t) \end{pmatrix}. \quad (2.8)$$

The time derivative of the resulting matrix is taken, and then it is multiplied on the left by the inverse of the rotation matrix, giving

$$\mathbb{G}^{-1} \cdot v(\mathbb{G} \cdot x) = \begin{pmatrix} \sigma y_1(t) - \sigma x_1(t) \\ \sigma y_2(t) - \sigma x_2(t) \\ -r_2 x_2(t) - y_1(t) - e y_2(t) + x_1(t)(r_1 - z(t)) \\ r_2 x_1(t) + e y_1(t) - y_2(t) + x_2(t)(r_1 - z(t)) \\ x_1(t) y_1(t) + x_2(t) y_2(t) - b z(t) \end{pmatrix}, \quad (2.9)$$

which is the same as the original system of ODEs, so that the system is rotationally equivariant for all finite angle rotations.

(R. Wilczak, Jun 19 2009)

## 2.5 Relative equilibria

**Exercise 2.10 Harmonic oscillator in polar coordinates:** Given a harmonic oscillator that follows  $\dot{p} = -q$  and  $\dot{q} = p$ , rewrite the system in polar coordinates and find equations for  $r$  and  $\theta$ .

**Solution 2.10 - Harmonic oscillator in polar coordinates.** Harmonic oscillator equations in Cartesian coordinates are

$$\dot{p} = -q, \quad \dot{q} = p. \quad (2.10)$$

In polar form, we write

$$q = r \cos \theta, \quad p = r \sin \theta. \quad (2.11)$$

The inverse of the Jacobian  $\frac{\partial\{q,p\}}{\partial\{r,\theta\}}$  of this transformation is

$$\frac{\partial\{r,\theta\}}{\partial\{q,p\}} = \begin{pmatrix} \cos \theta & \sin \theta \\ -\frac{1}{r} \sin \theta & \frac{1}{r} \cos \theta \end{pmatrix}, \quad (2.12)$$

leading to

$$\begin{pmatrix} \dot{r} \\ \dot{\theta} \end{pmatrix} = \begin{pmatrix} \cos \theta & \sin \theta \\ -\frac{1}{r} \sin \theta & \frac{1}{r} \cos \theta \end{pmatrix} \cdot \begin{pmatrix} \dot{q} \\ \dot{p} \end{pmatrix} = \begin{pmatrix} 0 \\ -1 \end{pmatrix} \quad (2.13)$$

(R. Wilczak, Jun 23 2009)

**Exercise 2.11 Complex Lorenz equations in polar coordinates.** Rewrite complex Lorenz equations from Cartesian to polar coordinates,

$$(x_1, x_2, y_1, y_2, z) = (\rho_1 \cos \theta_1, \rho_1 \sin \theta_1, \rho_2 \cos \theta_2, \rho_2 \sin \theta_2, z), \quad (2.14)$$

where  $\rho_1 \geq 0, \rho_2 \geq 0$ .

**Solution 2.11 - Complex Lorenz equations in polar coordinates.** We use the same method here as in exercise 2.10. The Jacobian of this transformation can be written as

$$\frac{\partial\{\rho_1, \theta_1, \rho_2, \theta_2, z\}}{\partial\{x_1, x_2, y_1, y_2, z\}} = \begin{pmatrix} \cos(\theta_1) & \sin(\theta_1) & 0 & 0 & 0 \\ -\frac{\rho_1}{\sin(\theta_1)} & \frac{\rho_1}{\cos(\theta_1)} & 0 & 0 & 0 \\ 0 & 0 & \cos(\theta_2) & \sin(\theta_2) & 0 \\ 0 & 0 & -\frac{\rho_2}{\sin(\theta_2)} & \frac{\rho_2}{\cos(\theta_2)} & 0 \\ 0 & 0 & 0 & 0 & 1 \end{pmatrix}. \quad (2.15)$$

Multiplying the velocity matrix on the left by the Jacobian (2.15), we get

$$\begin{pmatrix} \dot{\rho}_1 \\ \dot{\theta}_1 \\ \dot{\rho}_2 \\ \dot{\theta}_2 \\ \dot{z} \end{pmatrix} = \begin{pmatrix} -\sigma(\rho_1 - \rho_2 \cos \theta) \\ -\sigma \frac{\rho_2}{\rho_1} \sin \theta \\ -\rho_2 + \rho_1((r_1 - z) \cos \theta - r_2 \sin \theta) \\ e + \frac{\rho_1}{\rho_2}((r_1 - z) \sin \theta + r_2 \cos \theta) \\ -bz + \rho_1 \rho_2 \cos \theta \end{pmatrix},$$

where  $\theta = \theta_1 - \theta_2$ . Following ref. [1], we set  $r_2 = 0$  in what follows. It is convenient to rewrite this as 4 coupled equations

$$\begin{pmatrix} \dot{\rho}_1 \\ \dot{\rho}_2 \\ \dot{\theta} \\ \dot{z} \end{pmatrix} = \begin{pmatrix} -\sigma(\rho_1 - \rho_2 \cos \theta) \\ -\rho_2 + (r_1 - z)\rho_1 \cos \theta \\ -e - \left(\sigma \frac{\rho_2}{\rho_1} + (r_1 - z) \frac{\rho_1}{\rho_2}\right) \sin \theta \\ -bz + \rho_1 \rho_2 \cos \theta \end{pmatrix}, \quad (2.16)$$

and two driven ones for the two angles,

$$\begin{pmatrix} \dot{\theta}_1 \\ \dot{\theta}_2 \end{pmatrix} = \begin{pmatrix} -\sigma \frac{\rho_2}{\rho_1} \sin \theta \\ e + (r_1 - z) \frac{\rho_1}{\rho_2} \sin \theta \end{pmatrix}, \quad (2.17)$$

in agreement with ref. [1].

(R. Wilczak and P. Cvitanović, Jun 23 2009)

**Exercise 2.12 Visualizations of the complex Lorenz flow in polar coordinates:** Plot complex Lorenz flow projected on any three of the  $\{\rho_1, \rho_2, \theta, z\}$  coordinates. Experiment with different visualizations. The flow (2.16) is singular as  $\rho_j \rightarrow 0$ , with angle  $\theta_j$  going through a rapid change there: is that a problem? (See also exercise 2.20.) Does it make sense to insist on  $\rho_1 \geq 0, \rho_2 \geq 0$ , or should one let them have either sign in order that the  $\theta$  trajectory be continuous?

**Solution 2.12 - Visualizations of the complex Lorenz flow in polar coordinates.** (solution not available)

**Exercise 2.13 Computing the relative equilibrium  $Q_1$ :** Find the relative equilibria of the complex Lorenz equations by finding the equilibria of the system in polar coordinates (2.16). Compute the velocity of such relative equilibrium.

**Solution 2.13 - Computing the relative equilibrium  $Q_1$ .** A relative equilibrium point occurs when the derivatives (2.16) are equal to zero (so that the difference between the two angles  $\theta_1$  and  $\theta_2$  is constant, but the angles themselves are not constant). We use the `Solve` function (or the `Reduce` function) in `Mathematica` to find these points.

We define the system in `Solve` by setting all time derivatives in (2.16) to zero. `Mathematica` returns eight solutions of the form

$$\begin{aligned} z(t) &\rightarrow r_1 - 1 - \frac{e^2}{(\sigma + 1)^2} \\ \rho_2(t) &\rightarrow \pm \frac{\sqrt{e^2 + (\sigma + 1)^2} \sqrt{-b(e^2 - (r_1 - 1)(\sigma + 1)^2)}}{(\sigma + 1)^2} \\ \rho_1(t) &\rightarrow \pm \frac{\sqrt{-b(e^2 - (r_1 - 1)(\sigma + 1)^2)}}{\sqrt{(\sigma + 1)^2}} \\ \theta(t) &\rightarrow \pm \cos^{-1} \left( \pm \frac{\sqrt{(\sigma + 1)^2}}{\sqrt{e^2 + (\sigma + 1)^2}} \right) \end{aligned} \quad (2.18)$$

The solutions differ by combinations of negative and positive  $\rho_1$ ,  $\rho_2$ ,  $\theta$ . A negative  $\rho_i$  solution corresponds to the same group orbit of solutions, related to the positive  $\rho_i$  solution by a rotation by  $\pi$ . The  $\rho_1 \geq 0, \rho_2 \geq 0$  condition in (2.14) reduces these solutions to two, differing by the sign of  $\cos^{-1}$  term. Defining  $d = 1 + e^2/(\sigma + 1)^2$ , we can write them compactly as [1]

$$(\rho_1, \rho_2, \theta, z) = \left( \sqrt{b(r_1 - d)}, \sqrt{bd(r_1 - d)}, \pm \cos^{-1} \left( 1/\sqrt{d} \right), r_1 - d \right) \quad (2.19)$$

As will be further shown in exercise 2.15, these two solutions are equivalent. For the Siminos parameter values (1.3), the relative equilibrium is at

$$x_{Q_1} = (\rho_1, \rho_2, \theta, z) = (8.48527, 8.48562, 0.00909066, 26.9999) . \quad (2.20)$$

The angular velocity of relative equilibrium  $Q_1$  follows from (2.17). Both angles move with the same velocity

$$\dot{\theta}_i = \frac{\sigma e}{\sigma + 1} , \quad (2.21)$$

and period  $T_{Q_1} = 2\pi(\sigma + 1)/\sigma e$ .  $T_{Q_1} = 69.115 \dots$  for the Siminos parameter values (1.3). That implies that the simulation has to be run up to time of order 35 or higher for the strange attractor in figure 1.1 to start filling in. (R. Wilczak and P. Cvitanović, Jul 7 2009, Aug 7 2009)

**Exercise 2.14 Relative equilibrium  $Q_1$  in polar coordinates:** Plot the equilibrium  $Q_1$  in polar coordinates.

**Solution 2.14 - Relative equilibrium  $Q_1$  in polar coordinates.** The same method as in exercise (2.1) can be used here. First, a numerical solution is found with `NDSolve` for  $t$  going 0 to 10 and initial point  $Q_1$ . We again set `MaxSteps`  $\rightarrow$  `Infinity` in order to resolve the structure of the flow. Using `ParametricPlot3D` to plot the flow in  $\{\rho_1, \rho_2, z\}$  axes, Figure 1.4 illustrates the shape of the flow with parameters set to the Siminos values [1] (1.3).

(R. Wilczak, Jun 26 2009)

**Exercise 2.15** *Relative equilibrium  $Q_1$  in Cartesian coordinates:* Plot the relative equilibrium  $Q_1$  in Cartesian coordinates.

**Solution 2.15 - Relative equilibrium  $Q_1$  in Cartesian coordinates.** Using the same method as in exercise 2.14 and in exercise 2.1, we can plot the relative equilibrium in Cartesian coordinates. However, the Cartesian system is five-dimensional and our polar system has only four dimensions. To resolve this, we set  $\theta_2$  to an arbitrary value and set  $\theta_1 = \theta + \theta_2$ . With this, we can find the numerical value of  $Q_1$  in Cartesian coordinates using (2.14):

$$x_{Q_1} = (x_1, x_2, y_1, y_2, z) = (8.48492, 0.0771356, 8.48562, 0, 26.9999). \quad (2.22)$$

Using Mathematica to plot the system as before, but with  $t$  going from 0 to 100, figure 1.5(a) shows the complex Lorenz flow at  $Q_1$  projected onto the  $\{x_1, x_2, z\}$  subspace.

Note that for a relative equilibrium the flow is along a circle, i.e., the group-orbit of any point on it, but due to finite precision of the initial point and the integration, the trajectory eventually spirals away in a "horn" shape. This circle cuts through the middle of the complex Lorenz equations strange attractor, as shown in figure 1.5(b).

As noted in the solution to exercise 2.13, Mathematica returns eight relative equilibria, but they are all equivalent. Figure 1.6 shows the complex Lorenz flow starting near four of these eight points. Each of the points lies on the  $Q_1$  orbit, and each spirals away in the same way.

(R. Wilczak, Jun 26 2009)

**Exercise 2.16** *Eigenvalues and eigenvectors of  $Q_1$  stability matrix:* Compute the eigenvalues and eigenvectors of the stability matrix evaluated at  $Q_1$  and using the Siminos parameter values (1.3).

**Solution 2.16 - Eigenvalues and eigenvectors of  $Q_1$  stability matrix.** Using the Mathematica function `EigenSystem` and setting  $(\rho_1, \rho_2, \theta, z)(0)$  to the values in (2.20) we obtain

$$(\lambda_{1,2}, \lambda_3, \lambda_4) = (0.0938179 \pm 10.1945i, -11.0009, -13.8534)$$

as the eigenvalues of the system with the associated eigenvectors:

$$\begin{aligned} \operatorname{Re} e_1 &= (0.266121, -0.0321133, 0.00034139, 0.719222) \\ \operatorname{Im} e_1 &= (0.295017, 0.569063, 0.000551886, 0) \\ e_3 &= (-0.0883591, -0.0851485, -0.989135, -0.0809553) \\ e_4 &= (-0.855586, -0.329912, -0.00273531, -0.398902) \end{aligned} \quad (2.23)$$

The spiral-out instability appears very slow, but with a short period  $T_{\text{spiral}} = 0.6163$ , about 112 turns for one period of the  $Q_1$ . Actually, as the relative equilibrium velocity (2.21) is slow, an initial deviation from  $x_{Q_1}$  is multiplied by the factor  $\Lambda_{\text{radial}} = 535$ , and the relative equilibrium is quite unstable. This is illustrated by figure 1.5(b). It would be sweet if we could eliminate the detuning drift time scale  $\approx 70$  and focus just on the oscillatory time scale of  $\approx 0.6$ . That is one of the motivations for reformulating dynamics in a reduced state space. (R. Wilczak and P. Cvitanović, Jun 26 2009, Aug 7 2009)

**Exercise 2.17** *The eigen-system of  $Q_1$  stability matrix in polar coordinates:* Plot the eigenvectors of  $\mathbb{A}$  at  $Q_1$  in polar coordinates, as well as the complex Lorenz flow at values very near  $Q_1$ .

**Solution 2.17** - *The eigen-system of  $Q_1$  stability matrix in polar coordinates.* In order to plot the complex eigenvectors, we split them into their real and complex parts as in exercise 2.5. Using the same method as in the previous plotting exercises (exercise 2.1, exercise 2.15, exercise 2.14) we constructed Figure 1.7(a) and figure 1.7(b).

(R. Wilczak, Jul 01 2009)

## 2.6 Reduced state space

**Exercise 2.18** *SO(2) or harmonic oscillator slice:* Construct a moving frame slice for action of  $SO(2)$  on  $\mathbb{R}^2$

$$(x, y) \mapsto (x \cos \theta - y \sin \theta, x \sin \theta + y \cos \theta) \quad (2.24)$$

by, for instance, the positive  $y$  axis:  $x = 0, y > 0$ . Write out explicitly the group transformations that bring any point back to the slice. What invariant is preserved by this construction?  
(E. Siminos, Jun 26 2009)

**Solution 2.18** - *SO(2) or harmonic oscillator slice:* We can now construct a moving frame as follows. We write out explicitly the group transformations:

$$\bar{x} = x \cos \theta - y \sin \theta, \quad (2.25a)$$

$$\bar{y} = x \sin \theta + y \cos \theta. \quad (2.25b)$$

Then set  $\bar{x} = 0$  and solve (2.25a) for the group parameter to obtain the moving frame

$$\theta = \tan^{-1} \frac{x}{y} \quad (2.26)$$

which brings any point back to the slice. Substituting (2.26) in the remaining equation, we get the  $SO(2)$ -invariant expression

$$\bar{y} = \sqrt{x^2 + y^2}.$$

(E. Siminos, Jun 26 2009)

**Exercise 2.19** *State space reduction by a slice, finite time segments:* Replace integration of the complex Lorenz equations by a sequence of short time steps, each followed by a rotation such that the next segment initial point is in the slice  $x_2 = 0, x_1 > 0$ .

**Solution 2.19** - *State space reduction by a slice.* We start by setting the initial point and the time step that will be used during the integration. Using Mathematica, we first remove the  $z$  component of the initial point so that we have  $x(0) - x(0) \cdot \hat{z} =$

$\{x_1(0), x_2(0), y_1(0), y_2(0), 0\}$ . In order to rotate each of the points, we must construct a matrix

$$\mathbb{G} = \begin{pmatrix} \cos(\theta) & \sin(\theta) & 0 & 0 & 0 \\ -\sin(\theta) & \cos(\theta) & 0 & 0 & 0 \\ 0 & 0 & \cos(\theta) & \sin(\theta) & 0 \\ 0 & 0 & -\sin(\theta) & \cos(\theta) & 0 \\ 0 & 0 & 0 & 0 & 1 \end{pmatrix} \quad (2.27)$$

where  $\theta$  is the angle between the new point (minus the  $z$  component) and the positive  $x_1$  axis ( $\hat{x}_1 = \{1, 0, 0, 0, 0\}$ ). From exercise 2.8, we know that the complex Lorenz equations are invariant for this kind of rotation, so that when we reduce the complex Lorenz flow it contains the same information as the 5-dimensional system. We do not need to determine the angles themselves, we need only their cosines and sines. The cosine is found by a dot product as:

$$\cos(\theta) = \frac{x \cdot \hat{x}_1}{|x|} \quad (2.28)$$

Sines can be found by rotating each point by  $\frac{\pi}{2}$  and then taking the dot product as with cosine. Taking the first point, we first rotate it with  $\mathbb{G}$ , and starting with this rotated point, we integrate over the defined time step. We then take the last point from the integration, find its  $\mathbb{G}$  and rotate it, then use it at the beginning of the next integration from  $t = \text{timestep}$  to  $t = 2 \cdot \text{timestep}$ . This process continues (using a For loop in Mathematica) until the end of the integration (at an arbitrary time). The resulting list of rotated points is then plotted. Using this method, we produced figure 2.1(a) and figure 2.1(b).

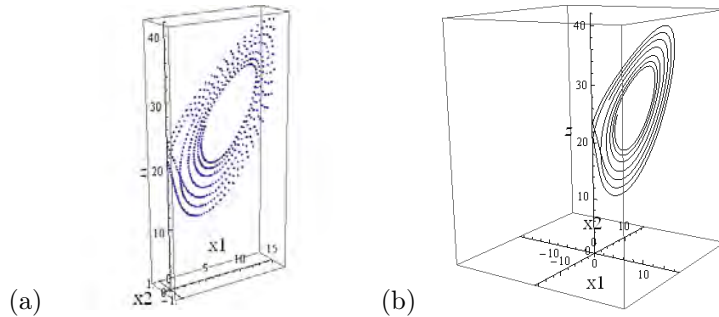


Figure 2.1: (a)  $\{x_1, x_2, z\}$  plot of the complex Lorenz flow as each point is rotated back to the plane. The time step used to make this plot was 0.01 and the integration went from  $t = 0$  to  $t = 50$ . (b) With the points connected into a curve.

(R. Wilczak, Jul 14 2009)

**Exercise 2.20** *Probability of hitting*  $(x_1, x_2) = (0, 0)$ : Investigate by simulation (and - that is extra cost - perhaps by thinking) how close does a strange attractor trajectory of complex Lorenz flow come to hitting  $(x_1, x_2) = (0, 0)$  and/or  $(y_1, y_2) = (0, 0)$ ?

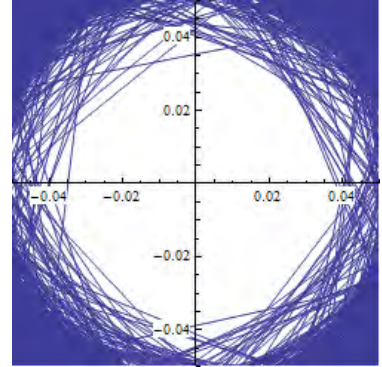


Figure 2.2: A very long time ( $t = 5000$ ) simulation of complex Lorenz flow.  $\{x_1, x_2\}$  plot indicates that probability of hitting  $(x_1, x_2) = (0, 0)$  is for all practical purposes equal to zero, and  $\sqrt{x_1^2 + x_2^2} > 0.02$ . (P. Cvitanović, Jul 14 2009)

**Solution 2.20 - Probability of hitting  $(x_1, x_2) = (0, 0)$ .** A very long time ( $t = 5000$ ) simulation of complex Lorenz flow, plot of  $\{x_1, x_2\}$  neighborhood in figure 2.2, indicates that probability of hitting  $(x_1, x_2) = (0, 0)$  is for all practical purposes equal to zero, and  $\rho_1(t) = \sqrt{x_1^2 + x_2^2} > 0.02$ . Plots of  $\{y_1, y_2\}$  neighborhood look similar. Hence reduction of state space to 4-dimensional  $x_2 = 0$  reduced state space by rotating successive trajectory increments back to the  $x_1 > 0$  semi-axis should not run into an  $x_1 = 0$  singularity in determining the rotation angle  $\cos \theta$ . (P. Cvitanović, Jul 14 2009)

**Exercise 2.21 State space reduction by a slice, ODE formulation:** Reconsider (2.19) in the sequence of infinitesimal time steps limit, each followed by an infinitesimal rotation such that the next segment initial point is in the slice  $x_2 = 0, x_1 > 0$ . Derive the corresponding 4d reduced state space ODE for the complex Lorenz flow.

**Solution 2.21 - State space reduction by a slice, ODE formulation:** Infinitesimal time version of the moving frames symmetry reduction is attained by taking small time steps in figure 1.8 and dropping the higher order terms, as in sect. 1.3:

$$dx^{(n)} = dt v(x^{(n)}) + d\theta_1^{(n)} \mathbb{T} \cdot x^{(n)}.$$

The infinitesimal angle is proportional to the time step,

$$\theta_1^{(n)} \approx \sin \theta_1^{(n)} = -dt \frac{\hat{e}_1 \cdot v(x^{(n)})}{\rho_1^{(n)}} \approx -dt v_1(x^{(n)})/x_2^{(n)},$$

where  $(\rho_1, \theta_1)$  are polar coordinates,  $\rho_1 = \sqrt{x_1^2 + x_2^2}$ , see (2.14). Our slice condition is  $x_1 = 0, x_2 > 0$ , so the reduced state space equations are given by

$$\dot{x} = v - \frac{v_1}{x_2} \mathbb{T} \cdot x. \quad (2.29)$$

The motion stays in the  $(d-1)$ -slice, as  $\dot{x}_1 = 0$  due to the orthogonal action of  $\mathbb{T}$  to the direction  $x$ .

CHAPTER 2. EXERCISES

---

Moving frames symmetry reduced complex Lorenz equations are a 4-dimensional first order ODE system

$$\begin{aligned}\dot{x}_2 &= -\sigma(x_2 - y_2) \\ \dot{y}_1 &= -y_1 + r_2 x_2 - (e + \sigma y_1/x_2) y_2 \\ \dot{y}_2 &= -y_2 + (r_1 - z)x_2 + (e + \sigma y_1/x_2) y_1 \\ \dot{z} &= -bz + x_2 y_2.\end{aligned}\tag{2.30}$$

The resulting trajectory is illustrated in figure 1.11. It agrees with trajectories reported by Siminos (there the simulation is in the full state space, and the reduced state space dynamics is obtained by a coordinate change).

- Checked that it agrees with finite step + rotation of figure 1.8
- $x_2$  and  $y_2$  seem locked, oscillate the same way with amplitude up to 20
- $y_1$  is very small, mostly below 0.1
- $(x_2, y_2, z)$  plot looks discontinuous in  $y_2$  whenever  $x_2$  small, across the  $z$ -axis (indicated in red). (R. Wilczak, Jul 28 2009)

**Exercise 2.22** *Accumulated phase shift in slice reduced state space:* Derive the 1d equation for the accumulated phase shift  $\theta$  associated with the 4d reduced state space ODE of exercise 2.21.

**Solution 2.22** - Accumulated phase shift in slice reduced state space: (not available)

**Exercise 2.23** *The moving frame flow stays in the reduced state space:* Show that the flow (1.18) stays in a  $(d-1)$ -dimensional slice. (P. Cvitanović, Aug 10 2009)

**Solution 2.23** - The moving frame flow stays in the reduced state space: The motion stays in the  $(d-1)$ -dimensional slice, as the flow along the group action direction vanishes,

$$\dot{x} \cdot \mathbb{T} \cdot x^* = v \cdot \mathbb{T} \cdot x^* - \frac{(v \cdot \mathbb{T} \cdot x^*)}{(x \cdot x^*)_4} (\mathbb{T} \cdot x) \cdot \mathbb{T} \cdot x^* = 0.$$

(P. Cvitanović, Aug 10 2009)

**Exercise 2.24** *Integration on a cross-section:* Siminos [1] replaces complex Lorenz equations with the system

$$\frac{dx}{dt} = \mathbf{P}^\perp(x^*)v(x), \quad \mathbf{P}_{ij}^\perp(x^*) = \delta_{ij} - \frac{(\mathbb{T} \cdot x^*)_i (\mathbb{T} \cdot x^*)_j}{(\mathbb{T} \cdot x^*)^2}\tag{2.31}$$

where  $x^*$  a point on the cross-section, solutions will stay on the cross-section  $\mathcal{K}$  for any initial condition on  $\mathcal{K}$  as there is no component of  $\mathbf{P}^\perp(x_o)v(x)$  in the direction of the continuous symmetry. Reproduce Siminos figure 1.12 (a). Explain the similarity to the classical 2-eared Lorenz attractor (note that dynamics on the slice are equivariant under rotations by  $\pi$ ).

**Solution 2.24 - Integration on a cross-section.** *Siminos [1] gives the new equation as*

$$\dot{x}_\perp = v(x) - \mathbb{T}x^* \frac{\mathbb{T}x^* \cdot v(x)}{(\mathbb{T}x^*)^2} \quad (2.32)$$

Using  $\mathbb{T} = \begin{pmatrix} 0 & 1 & 0 & 0 & 0 \\ -1 & 0 & 0 & 0 & 0 \\ 0 & 0 & 0 & 1 & 0 \\ 0 & 0 & -1 & 0 & 0 \\ 0 & 0 & 0 & 0 & 0 \end{pmatrix}$  and  $x^* = x_{Q1}$ , we can reproduce figure 1.12 (a) by

using the integration and plotting methods described in previous exercises. Our result is shown in figure 1.12 (b).

(R. Wilczak, Aug 07 2009)

# Chapter 3

## Open problems

Here we ponder where to go from Siminos thesis [1], investigate various ways of ‘quotienting’ the  $SO(2)$  symmetry in more general settings than the complex Lorenz equations. <sup>1</sup>

### 3.1 Complex Lorenz equations odds & ends

**Exercise 3.1** *Equilibria of complex Lorenz equations:* In exercise 2.3 we found only one equilibrium of complex Lorenz equations. The Ning and Haken [10] version of complex Lorenz equations (a truncation of Maxwell-Bloch equations describing a single mode ring laser) sets  $e + \rho_2 = 0$  so that a detuned equilibrium exists. Test your routines on 2 cases: (a)  $e = 0, \rho_2 = 0$ . As discussed by Siminos [1], reality of parameters  $a, \rho$  in (1.1) implies existence of a discrete  $C_2$  symmetry. (b)  $e + \rho_2 = 0, e \neq 0$ . You might want to compare results with those of Ning and Haken [10].

**Solution 3.1 - Equilibria of complex Lorenz equations.** (not available) (R. Wilczak, Jul ?? 2009)

#### 3.1.1 $SO(2)$ invariants of complex Lorenz equations

**Predrag - July 6 2009:**

The generators (Lie algebra elements) of  $SO(n)$  rotations are antisymmetric (cf. (2.5)),  $v(x) \cdot \mathbb{T} \cdot v(x) = 0$ , so from (1.10) it follows that

$$0 = v(x) \cdot \frac{dv}{dx} \cdot \mathbb{T} \cdot x. \quad (3.1)$$

This would appear to be a nontrivial multinomial relation between the 5 coordinates of complex Lorenz equations, but **Mathematica** evaluation shows that

---

<sup>1</sup>wilczak/blog/open.tex, rev. 53: last edit by Predrag Cvitanović, 08/13/2009

it is identically satisfied by the dynamical equations, yielding no constraint on dynamics.

Noether's theorem suggests that a conserved (invariant) quantity should be associated with each 1-parameter continuous invariance [11], i.e., it should be possible to write a "Hamiltonian," in terms of "momentum, angle" variables such that the "momentum" variable (radius  $r$  in the harmonic oscillator of example 2.10) is conserved, and the conjugate angle variable has trivial dynamics.

We do not know how to construct such invariant function, but due to the length conservation under rotations (antisymmetry of the Lie algebra generators such as (2.5)), functions such as  $R_{E_0}^2 = (x - x_{E_0}) \cdot (x - x_{E_0})$

$$\frac{d}{d\theta} R_{E_0}^2 = (x - x_{E_0}) \cdot \mathbb{T} \cdot (x - x_{E_0}) = 0 \quad (3.2)$$

are invariant.

## 3.2 A flow with two Fourier modes

**Predrag - Jul 9 2009:**

Complex Lorenz equations (1.1) of Gibbon and McGuinness [2] have a degenerate 4-dimensional subspace, with  $SO(2)$  acting only in its lowest non-trivial representation. Here is a possible model, still 5-dimensional, but with  $SO(2)$  acting in the two lowest representations. Such models arise as truncations of Fourier-basis representations of PDEs on periodic domains. In the complex form, the simplest such modification of complex Lorenz equations may be the "2-mode" system

$$\begin{aligned} \dot{x} &= -\sigma x + \sigma x^* y, \\ \dot{y} &= (r - z)x^2 - ay, \\ \dot{z} &= \frac{1}{2} (x^2 y^* + x^{*2} y) - bz, \end{aligned} \quad (3.3)$$

where  $x, y, r = r_1 + i r_2, a = 1 + i e$  are complex and  $z, b, \sigma$  are real. Rewritten in terms of real variables  $x = x_1 + i x_2, y = y_1 + i y_2$  this is a 5-dimensional first order ODE system

$$\begin{aligned} \dot{x}_1 &= -\sigma x_1 + \sigma y_1, \\ \dot{x}_2 &= -\sigma x_2 + \sigma y_2, \\ \dot{y}_1 &= (r_1 - z)x_1 - r_2 x_2 - y_1 - e y_2, \\ \dot{y}_2 &= r_2 x_1 + (r_1 - z)x_2 + e y_1 - y_2, \\ \dot{z} &= -bz + x_1 y_1 + x_2 y_2. \end{aligned} \quad (3.4)$$

**Exercise 3.2 2-mode system in terms of real variables:** Verify (3.4) by substituting  $x = x_1 + i x_2, y = y_1 + i y_2, r = r_1 + i r_2, a = 1 + i e$  into the complex 2-mode equations (3.3).

**Solution 3.2 - 2-mode system in terms of real variables.** (solution not available)

### 3.2.1 Visualizing 2-mode system

**Exercise 3.3** *Visualizations of the 5-dimensional 2-mode system:* Plot 2-mode system projected on any three of the five  $\{x_1, x_2, y_1, y_2, z\}$  axes. Experiment with different visualizations. It's a big mess - have no clue what parameters to take, what the trajectory will do.

**Solution 3.3** - Visualizations of the 5-dimensional 2-mode system. (solution not available)

Figure 3.1:  $\{x_1, x_2, z\}$  plot of 2-mode system, with initial point  $(x_1, x_2, y_1, y_2, z) = (1, 0, 0, 1, 1)$ .

## 3.3 Linear stability

**Exercise 3.4** *Stability matrix of 2-mode system:* Find the stability matrix of 2-mode system (3.4).

**Solution 3.4** - Stability matrix of 2-mode system: (solution not available)

## 3.4 Symmetries of dynamics

### 3.4.1 Rotational equivariance of 2-mode system

**Exercise 3.5**  *$U(1)$  equivariance of 2-mode system for finite angles:* Show that 2-mode system (3.3) is equivariant under rotation for finite angles.

**Solution 3.5** -  $U(1)$  equivariance of complex Lorenz equations for finite angles. Obvious by inspection; that's how the equations (3.3) were constructed in the first place.

**Exercise 3.6**  *$SO(2)$  equivariance of the 2-mode system for finite angles:* Show that the 2-mode system is equivariant under rotation for finite angles.

**Solution 3.6** -  $SO(2)$  equivariance of the 2-mode system for finite angles. (solution not available)

**Exercise 3.7**  *$SO(2)$  equivariance of the 2-mode system for infinitesimal angles.* Show that the 2-mode system is equivariant under rotation for infinitesimal angles.

**Solution 3.7** - **SO(2) equivariance of the 2-mode system for infinitesimal angles.** We can check the equivariance condition (1.10),  $0 = -\mathbb{T}v(x) + \mathbb{A}\mathbb{T}x$ , where  $\mathbb{A} = \frac{\partial v}{\partial x}$  is the stability matrix, by explicit substitution. The matrix  $\mathbb{T}$  is

$$\mathbb{T} = \begin{pmatrix} 0 & 1 & 0 & 0 & 0 \\ -1 & 0 & 0 & 0 & 0 \\ 0 & 0 & 0 & 2 & 0 \\ 0 & 0 & -2 & 0 & 0 \\ 0 & 0 & 0 & 0 & 0 \end{pmatrix}. \quad (3.5)$$

Plugging these into (1.10) and using (3.4) for  $v(x)$  should yield a zero vector. .

## 3.5 Equilibria

An equilibrium is any point for which the velocity field of an ordinary differential equation is zero.

**Exercise 3.8** *Equilibria of 2-mode system:* Find all equilibria of 2-mode system.

**Solution 3.8** - **Equilibria of 2-mode system.** (solution not available)

## 3.6 Relative equilibria

### 3.6.1 Equations in the polar form

**Exercise 3.9** *2-mode system in polar coordinates.* Rewrite 2-mode system from Cartesian to polar coordinates,

$$(x_1, x_2, y_1, y_2, z) = (\rho_1 \cos \theta_1, \rho_1 \sin \theta_1, \rho_2 \cos \theta_2, \rho_2 \sin \theta_2, z), \quad (3.6)$$

where  $\rho_1 \geq 0, \rho_2 \geq 0$ .

**Solution 3.9** - **2-mode system in polar coordinates.** (solution not available)

### 3.6.2 Computing and plotting the relative equilibrium $Q_1$

**Exercise 3.10** *Computing the relative equilibrium  $Q_1$ :* Find the relative equilibria of the 2-mode system by finding the equilibria of the system in polar coordinates (2.16).

**Solution 3.10** - **Computing the relative equilibrium  $Q_1$ .** (solution not available)

**Exercise 3.11** *Plotting relative equilibrium  $Q_1$  in polar coordinates:* Plot the equilibrium  $Q_1$  in polar coordinates.

**Solution 3.11** - Plotting relative equilibrium  $Q_1$  in polar coordinates. (*solution not available*)

**Exercise 3.12** *Plotting relative equilibrium  $Q_1$  in Cartesian coordinates:* Plot the relative equilibrium  $Q_1$  in Cartesian coordinates.

**Solution 3.12** - Plotting relative equilibrium  $Q_1$  in Cartesian coordinates. (*solution not available*)

### 3.6.3 Eigenvalues and eigenvectors of the stability matrix

**Exercise 3.13** *Eigenvalues and eigenvectors of  $E_0$  stability matrix:* Find the eigenvalues and the eigenvectors of the stability matrix  $\mathbb{A}$  at  $E_0$ .

**Solution 3.15** - Eigenvalues and eigenvectors of  $E_0$  stability matrix. (*solution not available*)

**Exercise 3.14** *Plotting the eigenvalues and eigenvectors of the stability matrix at  $E_0$ :* Plot the eigenvectors of  $\mathbb{A}$  at  $E_0$  and the 2-mode system at values very close to  $E_0$ .

**Solution 3.14** - Plotting the eigenvalues and eigenvectors of the stability matrix at  $E_0$ : (*solution not available*)

**Exercise 3.15** *Finding the eigenvalues and eigenvectors of  $Q_1$  stability matrix:* Compute the eigenvalues and eigenvectors of the stability matrix evaluated at  $Q_1$  and using the Siminos thesis values (1.3).

**Solution 3.15** - Finding the eigenvalues and eigenvectors of  $Q_1$  stability matrix. (*solution not available*)

**Exercise 3.16** *Plotting the eigenvalues and eigenvectors of the stability matrix at  $Q_1$  in polar coordinates:* Plot the eigenvectors of  $\mathbb{A}$  at  $Q_1$  in polar coordinates, as well as the polar 2-mode system at values very near  $Q_1$ .

**Solution 3.16** - Plotting the eigenvalues and eigenvectors of the stability matrix at  $Q_1$  in polar coordinates. (*solution not available*)

# Bibliography

- [1] E. Siminos. *Recurrent spatio-temporal structures in presence of continuous symmetries*. PhD thesis, School of Physics, Georgia Institute of Technology, Atlanta, 2009.  
[ChaosBook.org/projects/theses.html](http://ChaosBook.org/projects/theses.html).
- [2] J.D. Gibbon and M.J. McGuinness. The real and complex Lorenz equations in rotating fluids and lasers. *Physica D*, 4:139, 1982.
- [3] J. F. Gibson, J. Halcrow, and P. Cvitanović. Visualizing the geometry of state-space in plane Couette flow. *J Fluid Mech.*, 611:107–130, 2008.  
[arXiv:0705.3957](https://arxiv.org/abs/0705.3957).
- [4] J. F. Gibson. Movies of plane Couette. Technical report, Georgia Institute of Technology, 2008. [ChaosBook.org/tutorials](http://ChaosBook.org/tutorials).
- [5] P. Cvitanović, R. Artuso, R. Mainieri, G. Tanner, and G. Vattay. *Chaos: Classical and Quantum*. Niels Bohr Institute, Copenhagen, 2009. [ChaosBook.org](http://ChaosBook.org).
- [6] É. Cartan. La méthode du repère mobile, la théorie des groupes continus, et les espaces généralisés. *Exposés de Géométrie*, 5, 1935.
- [7] M. Fels and P. J. Olver. Moving coframes: I. A practical algorithm. *Acta Appl. Math.*, 51:161, 1998.
- [8] M. Fels and P. J. Olver. Moving coframes: II. Regularization and theoretical foundations. *Acta Appl. Math.*, 55:127, 1999.
- [9] P. J. Olver. *Classical Invariant Theory*. Cambridge University Press, Cambridge, 1999.
- [10] C. Ning and H. Haken. Detuned lasers and the complex Lorenz equations: Subcritical and supercritical Hopf bifurcations. *Physica D*, 4:139, 1982.
- [11] V. I. Arnol'd. *Mathematical Methods for Classical Mechanics*. Springer, New York, 1989.